J. Membrane Biol. 166, 51–59 (1998)

The Journal of
Membrane
Biology

Electrocoupling of Ion Transporters in Plants: Interaction with Internal Ion Concentrations

D. Gradmann[1], **J. Hoffstadt**[2]

[1]Abteilung Biophysik der Pflanze, Albrecht-von-Haller-Institut für Pflanzenwissenschaften, Universität Göttingen, Untere Karspüle 2, D-37073 Göttingen, Germany

[2]Institut für Pflanzenökologie, Justus-Liebig-Universität, Heinrich-Buff-Ring 38, D-35392 Giessen, Germany

Received: 23 February/Revised: 16 July 1998

Abstract. There are five major electroenzymes in the plasmalemma of plant cells: a driving electrogenic pump, inward and outward rectifying K^+ channels, a Cl^--$2H^+$ symporter, and Cl^--channels. It has been demonstrated previously (Gradmann, Blatt & Thiel 1993, *J. Membrane Biol.* **136:**327–332) how voltage-gating of these electroenzymes causes oscillations of the transmembrane voltage (*V*) at constant substrate concentrations. The purpose of this study is to examine the interaction of the same transporter ensemble with cytoplasmic concentrations of K^+ and Cl^-. The former model system has been extended to account for changing internal concentrations. Constant-field theory has been applied to describe the influence of ion concentrations on current-voltage relationships of the active channels. The extended model is investigated using a reference set of model parameters. In this configuration, the system converges to stable slow oscillations with intrinsic changes in cytoplasmic K^+ and Cl^- concentrations. These slow oscillations reflect alternation between a state of salt uptake at steady negative values of *V* and a state of net salt loss at rapidly oscillating *V*, the latter being analogous to the previously reported oscillations. By switching off either concentration changes or gating, it is demonstrated that the fast oscillations are mostly due to the gating properties of the Cl^- channel, whereas the slow oscillations are controlled by the effect of the Cl^- concentration on the current. The sensitivity of output results *y* (e.g., frequency of oscillations) to changes of the model parameters *x* (e.g., maximum Cl^- conductance) has been investigated for the reference system. Further examples are presented where some larger changes of specific model parameters cause fundamentally different behavior, e.g., convergence towards a stable state of only the fast oscillations without intrinsic concentration changes, or to a steady-state without any oscillations. The main and general result of this study is that the osmotic status of a plant cell is stabilized by the ensemble of familiar electroenzymes through oscillatory interactions with the internal concentrations of the most abundant ions. This convergent behavior of the stand-alone system is an important prerequisite for osmotic regulation by means of other physiological mechanisms, like second messengers and gating modifiers.

Key words: Electrocoupling — Interactions — Ionic relations — Gating model — Plant membranes — Voltage oscillations

Introduction

Previous studies have treated oscillatory interactions of ion transporters in the membrane of plant cells during periods short enough to ignore changes of the internal concentrations of the major ions K^+ and Cl^- (Gradmann et al., 1993; Thiel & Gradmann, 1994; Gradmann & Buschmann, 1996; Buschmann & Gradmann, 1997). In those studies, the individual ion transporters could be assumed to have a constant electromotive force. Another simplification in those studies was to assume ohmic conductances for the active transporters. This assumption reflected the frequent ignorance of the shape of the current-voltage relationships (*IV* curves) of the transporters, where both super- and sublinearities are possible. For the point of those studies, most physiological issues, such as metabolism, signal tranduction, or compartmentation, have been ignored.

The success of those studies in explaining observed

Correspondence to: D. Gradmann

voltage oscillations with a rather minimal model might lead to the expectation that it is simply a matter of incorporating some of the missing physiological processes mentioned above, in order to arrive at a realistically behaving model that can subsequently be used to deduce physiological properties from experimental observations. Apart from the fact that this inverse modeling is a serious mathematical challenge even when dealing with far less complex systems (Tarantola, 1987), we hold the view that one has to know, or assume, much of these properties a priori to come up with a process description in the first place.

We believe that current knowledge about these processes is not sufficient to attempt building such a complex model. We could expect such a model to have so many degrees of freedom, that its sheer complexity would limit our insight into the regulation and feedbacks at work in plant cells to what we suspect already. Instead, we concentrate on studying manageable subsystems, which provides a basic understanding of the system's building blocks, and still offers testable predictions to experimentalists.

In this sense, the previous work demonstrated that the minimal ensemble of ion transporters alone could account for observed voltage oscillations. The question is now, can this ensemble also account for the regulation of major ion concentrations? Which is the minimal system that leads to a reliable, stable osmotic state?

The aim of this study is therefore to assess the interaction between the ensemble of the electroenzymes in the membrane and the concentrations of their ionic substrates in the cells. For this purpose, the previous model has been extended to account for substantial changes of the internal concentrations of K^+ and Cl^-. The first attempt revealed that the previous model exhibits unstable behavior with ion concentrations approaching either zero or infinity in most cases (*data not shown*). This diverging behavior could be ascribed to the assumption of linear current-voltage relationships for the transporters, which did not matter for the original system where equilibrium potentials were fixed anyway, but which is now clearly inappropriate for the system in question. This observation led us to assume that the (nonlinear) currents through open channels follow the constant field theory for independent electrodiffusion of ions through membranes, known as Goldman-Hodgkin-Katz relationships (*GHK*). The other simplifications (such as a minimal set of substrates, electroenzymes and states of activity) are the same here as in the previous model (Gradmann et al., 1993).

For the numerical treatment of this problem we started with model parameters which have originally been chosen to describe oscillations of the transmembrane voltage, *V*, in guard cells (Gradmann et al., 1993). Therefore, the results presented here will reflect the properties of guard cells relatively well compared with other cells. Because of the mentioned simplifications, however, these isolated model calculations cannot yield reliable predictions about the detailed behavior of a guard cell. On the other hand, these calculations demonstrate a fundamental mechanism which we expect to be valid not only for guard cells but for plant cells in general. This mechanism assures that the intrinsic interaction between the most common electroenzymes in the membrane and cytoplasmic concentrations of their ionic substrates lead the cell into a stable oscillatory state in which homeostasis of the internal concentrations is maintained, regardless of additional stabilizing and regulating influences of other physiological processes.

Theory

Figure 1 illustrates the model we used. The kidney-shaped contour represents a guard cell. It is assumed to have a well buffered internal (cytoplasmic, *c*) pH_c = constant, and an area/volume ratio of about 10^6 m^{-1}. For external (luminal, *l*) conditions, we assumed a constant pH_l of 6.0 and constant concentrations of K^+ and Cl^- ($c_{K,l} = c_{Cl,l} = 1$ mM), due to a large volume ratio between the environmental compartment and the cytoplasmic one. Electrophysiologically, the plasmalemma can be characterized by five major transporters with nonlinear and time-dependent conductances *g* as well as equilibrium voltages *E* which depend on the ratios of the corresponding substrate(s) inside and outside. These five pathways represent the known major mechanisms for charge carrying uptake and release of cations and anions: an electrogenic pump (*Pu*, usually a H^+ ATPase) which drives the internal voltage (*V*) negative with respect to outside, outward rectifying K^+ channels (K_o), inward rectifying K^+ channels (K_i), a Cl^--$2H^+$ symporter (*Sy*) for Cl^- uptake (this symporter is still to be identified in guard cells but known from other plant cells), and Cl^- channels (*Cl*). The equilibrium voltages of the pathways are (at 20°C):

$$\begin{aligned} E_{Pu} &= \Delta G_{ATP}/F + E_H \\ &= \Delta G_{ATP}/F + (-59\ \text{mV}) \cdot \log(c_{H,c}/c_{H,l}) \\ &\approx -400\ \text{mV} \end{aligned} \qquad (1a,b,c)$$

where ΔG_{ATP} is the free energy of ATP hydrolysis and *F* the Faraday constant,

$$E_{Ki} = E_{Ko} = E_K = (-59\ \text{mV}) \cdot \log\,(c_{K,c}/c_{K,l}) \qquad (2a,b,c)$$

$$\begin{aligned} E_{Sy} &= (-59\ \text{mV}) \cdot \log(c_{H,c}{}^2 \cdot c_{Cl,c}/(c_{H,I}{}^2 \cdot c_{Cl,l})) \\ &= (-59\ \text{mV}) \cdot (\log(c_{Cl,c}/c_{Cl,l}) + 2\Delta\text{pH}) \end{aligned} \qquad (3a,b)$$

$$E_{Cl} = (59\ \text{mV}) \cdot \log(c_{Cl,c}/c_{Cl,l}), \qquad (4)$$

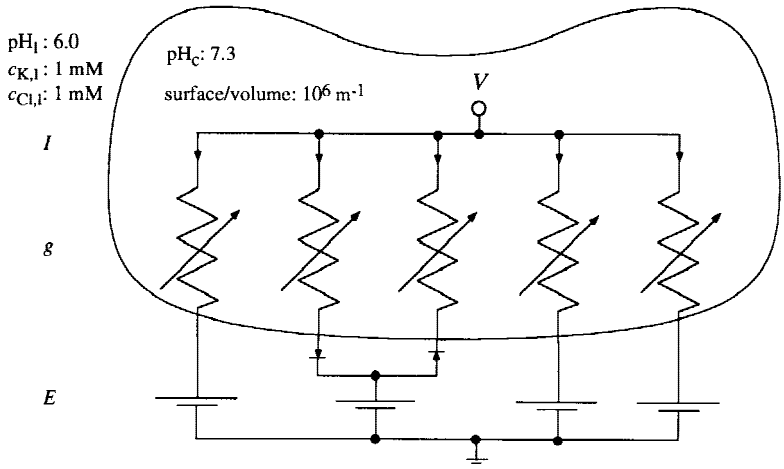

Transporter	*Pu*	K_o	K_i	*Sy*	*Cl*
E / (-59 mV)	400 / 59	$\lg \frac{c_{K,c}}{c_{K,l}}$		$\lg \frac{c_{Cl,c}}{c_{Cl,l}} + 2\Delta pH$	$-\lg \frac{c_{Cl,c}}{c_{Cl,l}}$
IV_{active}	Ω	*GHK*		Ω	*GHK*
g_{mx}/Sm^{-2}	1	0.1 mM^{-1}	0.2 mM^{-1}	0.65	0.1 mM^{-1}
$k_{a,i}$/s^{-1} ($f = e^{u/2}$)	$a \underset{10f}{\overset{1/f}{\rightleftharpoons}} i$	$a \underset{1/f}{\overset{1f}{\rightleftharpoons}} i$	$a \underset{100f}{\overset{1/f}{\rightleftharpoons}} i$	$a \underset{1f}{\overset{1/f}{\rightleftharpoons}} i$	$i_1 \underset{25f}{\overset{0.5/f}{\rightleftharpoons}} a \underset{1f}{\overset{0.1/f}{\rightleftharpoons}} i_2$

Fig. 1. Simplified analogue circuit of the plasmalemma of a guard cells; five major ion transport systems: *Pu:* H^+ ATPase, K_o*:* outward rectifying K^+ channel, K_i*:* inward rectifying K^+ channel, *Sy:* Cl^--$2H^+$ symporter, *Cl:* Cl^- channel; *E:* equilibrium voltages at 20°C, $\Delta pH = pH_c - pH_l$; IV_{active} (current-voltage characteristics of active transport system): Ω: linear (ohmic), *GHK:* constant-field approach (Goldman-Hodgkin-Katz); g_{mx}*:* membrane conductance of fully active system, for *Pu* and *Sy* in $S \cdot m^{-2}$, and for channels (K_i, K_o, and *Cl*) in $S \cdot m^{-2}$ at 1 mM substrate concentration on both sides of the membrane; $k_{a,i}$*:* voltage-sensitive rate constants (transition probabilities) for transition k_a from inactive to active state and for k_i from inactive to active state of transport systems; simplified voltage-sensitivities: multiplication or division of listed k's at $V = 0$ mV by $f = e^{u/2}$.

where $c_{K,c}$ and $c_{Cl,c}$ are free to change, while the other substrate concentrations, $c_{K,l}$, $c_{Cl,l}$, $c_{H,c}$, $c_{H,l}$, and ΔG_{ATP} are assumed to be constant either due to large reservoirs or due to buffering.

The current density through each transporter ensemble is

$$I_i = g_i (V - E_i) \tag{5}$$

where the membrane conductances g_i may be voltage-sensitive. Since the shapes of the steady-state current-voltage relationships (*IV*) of the active transporters are not known in general, two simplifying approaches are used here, i.e., voltage-insensitive g ('ohmic',Ω) or voltage-sensitive g as predicted by the Goldman-Hodgkin-Katz constant-field current equation (*GHK*), which can be written in the form

$$I_{GHK} = g^o V \frac{c_c - c_l e^{-zu}}{1 - e^{-zu}} \tag{6}$$

with the voltage-insensitive conductance g^o for reference concentrations (1 mM) in the cytoplasm (c_c) and in the lumen (c_l), and the reduced membrane voltage $u = VF/(RT)$, where z, R, and T have their usual thermodynamic meanings.

The *GHK*-approach has been applied here only to the channels. *IV* of the active pump is treated as a battery with constant electromotive force and voltage-insensitive conductance because changes in E_{Pu} and g_{Pu} of the active pump cannot be expected within the framework of this model due to buffering of pH_c, constant pH_l and the absence of immediate effects on ΔG_{ATP}. As for the symporter, E_{Sy} changes according to Eq.(3), whereas g of the active symporter is assumed to be linear and constant in this context, first because the shape of the *IV*-curve of the active symporter is not known and secondly because, under the conditions investigated here, the symporter operates (almost) exclusively in the Cl^- uptake direction at constant $c_{Cl,l}$, and changes in $c_{Cl,c}$ will have no significant effect on the investigated symporter currents.

Voltage-gating of the five pathways is treated here in the same simplifying way as previously (Gradmann et al., 1993). Briefly, each of the five transporters (except *Cl*) alternates between an active state (a) and an inactive state (i) with a symmetric energy barrier in between, where the transition probabilities $k_a = k_{i \to a}$ and $k_i = k_{a \to i}$ depend on the membrane voltage in the form

$$k_a = k_a^0 \cdot \exp(d_a u), \tag{7a}$$

$$k_i = k_i^0 \cdot \exp(d_i u), \tag{7b}$$

where the superscript ^{0} marks $k_{a,i}$ at zero voltage and the

voltage-sensitivity coefficients $d_{a,i} = \delta_{a,i} z\Delta$ comprise the electrical distances $\delta_{a,i}$ ($0 < \delta_a < 1$, $\delta_i = \delta_a - 1$; we assumed symmetry where $\delta_a = 0.5$ and $\delta_i = -0.5$) of the peak of the barrier with the electrical width 1 between the adjacent energy wells (cytoplasmic side: 0), and the charge z of the gating particle which moves along the portion Δ of the entire membrane voltage. Frequently, the non-integer parameter $d = d_a - d_i$ is called 'gating charge'.

For the two-state transporters, the occupancies of the active state, p_a, and of the inactive state, p_i, change due to first-order processes of activation and inactivation, so that

$$dp_a/dt = k_a p_i - k_i p_a = -dp_i/dt \qquad (8a,b)$$

Since $p_a + p_i = 1$, it is sufficient to account for p_a only. If V remains unchanged, the steady-state activity, p_a ($0 < p_a < 1$), is

$$p_a = \frac{k_a}{k_a + k_i} = \frac{1}{1 + K_I exp(du)} = \frac{1}{1 + exp(d(u - u_{1/2}))} \qquad (9a,b,c)$$

with the stability constant $K_I = k_i/k_a = k_i^0/k_a^0$ for the inactive state and the reduced 'gating-V', $u_{1/2} = 1nK_A (K_A = 1/K_I)$, for half maximum activity at $k_i = k_a$.

The Cl^- transporter can change from the active state a into either of two inactive states, i_1 or i_2. The differential equations of the corresponding reaction scheme, $i_1 - a - i_2$, are

$$dp_{i1}/dt = -k_{a1} p_{i1} + k_{i1} p_a \qquad (10a)$$

$$dp_a/dt = k_{a1} p_{i1} - (k_{i1} + k_{i2}) p_a + k_{a2} p_{i2} \qquad (10b)$$

$$dp_{i2}/dt = k_{i2} p_a - k_{a2} p_{i2} \qquad (10c)$$

From this, the steady-state occupancies

$$p_a(Cl) = k_{a1} \cdot k_{a2}/den \qquad (11a)$$

$$p_{i1}(Cl) = k_{a2} \cdot k_{i1}/den \qquad (11b)$$

$$p_{i2}(Cl) = k_{a1} \cdot k_{i2}/den \qquad (11c)$$

can be derived with

$$den = k_{a1} \cdot k_{a2} + k_{a2} \cdot k_{il} + k_{a1} \cdot k_{i2}. \qquad (12)$$

The effective current density I_i through a pathway i is

$$I_i = I_{a,i} \cdot P_{a,i}, \qquad (13)$$

the product of the current density $I_{a,i}$ which would flow if the entire ensemble of type i transporters were active, and the actual portion $p_{a,i}$ ($0 < p < 1$), of this ensemble being active.

The free running voltage will adjust to a value $V_{I=0}$ where the sum of the current densities, ΣI_i, vanishes. For our calculations in the time range >> 1 msec, the membrane capacitance can be neglected. Test runs of the model program with and without a membrane capacitance of 10 $mF \cdot m^{-2}$ showed only a capacitance-induced damping of the peaks of the V-tracings by <5%. To determine $V_{I=0}$ we calculate the momentary IV relationship of the total system with $I = \Sigma I_i$ which is monotonic with a positive slope because each momentary I_i rises monotonically with V as well in both models (Ω and GHK). So $V_{I=0}$ can easily be determined by iterative bracketing and bisectioning when the initial range of current densities comprises both signs.

From the individual current densities I_i ($V_{I=0}$) at this voltage, the effluxes $J_i = I_i/(z_i F)$ in $mol \cdot m^{-2} \cdot s^{-1}$ of the substrates can readily be determined as well as the corresponding changes $dc_{i,c}/dt = J_i \cdot R_{A:V}$ of the cytoplasmic substrate concentrations at a given area/volume ratio $R_{A:V}$.

The entire model consists of a set of differential equations which describe the changes of ion concentrations and of state occupancies for the transporters with time. So, with a given start configuration of cytoplasmic concentrations (and the assumption of constant external concentrations), the temporal changes of $c_{i,c}$ could be calculated iteratively using small steps in Δt. At any given time and system state, one can calculate the equilibrium voltages E_i from the momentary ion concentrations, the currents I_i, and the membrane voltage V from the momentary occupancies. From this the time derivatives, dp/dt (Eqs. 8 and 10), can be determined. For the numerical integration, fixed-step Euler procedures have been used, as well as Runge-Kutta methods of second and fourth order with Δt in the order of 1 msec. Only those results have been accepted which yielded virtually identical results when Δt was varied by a factor of 2. The computer programs for this study and related subjects are available on request.

Results and Discussion

The numerical parameters given in Fig. 1 served as a reference set to discuss the properties of the model. Establishing this set of parameters started from the standard parameter set of the preceding model (Gradmann et al., 1993) when every active transporter has been treated as a battery with constant electromotive force and ohmic inner resistance. The parameters were modified through trial and error to examine the behavior of the system. The orders of magnitude have been balanced to avoid completely unrealistic values or time

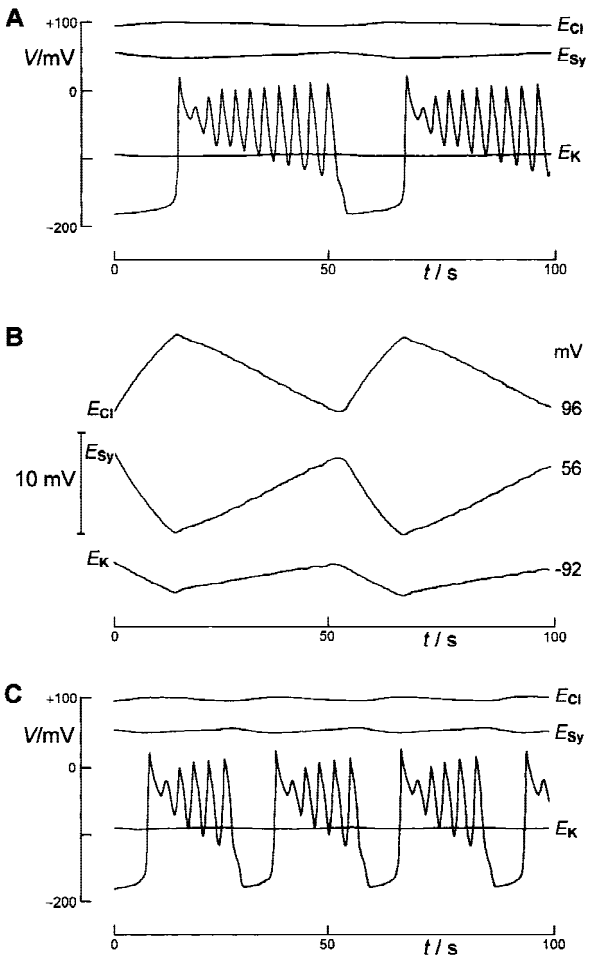

Fig. 2. Temporal characteristic of model with parameters in Fig. 1; cytoplasmic start concentrations: 37 mM K^+, and 42.8 mM Cl^-; (*A*) Time courses of free running voltage and of equilibrium voltages E_K, E_{Sy} and E_{Cl}; common voltage scale for comparison; (*B*) Time courses of E_K, E_{Sy} and E_{Cl} as in *A* with expanded voltage scale; (*C*) Same as *A*, except doubled area/volume ratio ($2 \cdot 10^6$ m^{-1}).

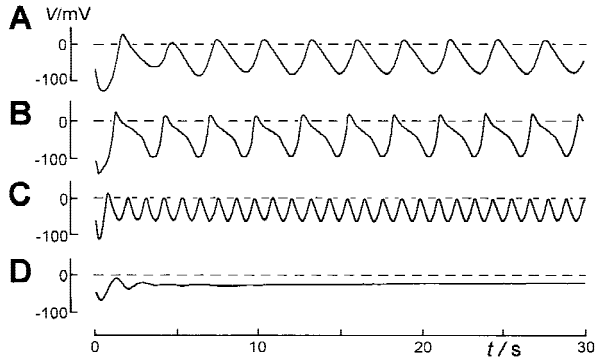

Fig. 3. Effects of specific configurations of the rate constants *k* in the model system Fig. 1 on fast oscillations, under conditions when slow oscillations are absent due $c_{K,c}$ = const (=20 mM) and $c_{Cl,c}$ = const (=60 mM); start with parameters for V = 0 mV; (*A*) with reference parameters as in Fig. 1; (*B*) with doubled values for *k*s of *Pu*, K_o, K_i, and *Sy* compared to *A*, showing no major change in frequency: (*C*) same as *B* but three times larger *k*s of *Cl* as in *A* and *B*, showing (almost) three-times increased frequency; (*D*) same as *A* but three times larger *k*s of *Cl*, showing damped oscillations of about three times higher frequency.

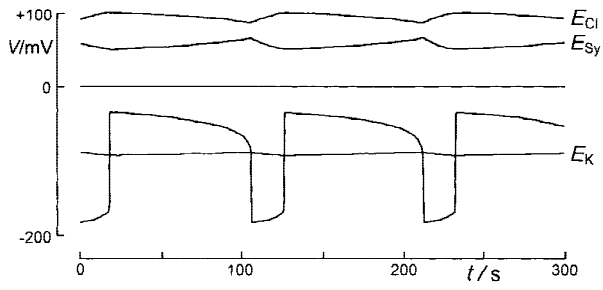

Fig. 4. Temporal behavior of the model system (Fig. 1) with reference parameters, except temporal relaxations of voltage-sensitive gating replaced by immediate, voltage-sensitive activities, showing persistence of slow oscillations with intrinsic changes of cytoplasmic ion concentrations, and absence of fast oscillations.

scales, but due to the simple nature of the model we did not attempt to tune parameters to produce experimentally observed concentrations or time courses.

Slow and Fast Oscillations

The temporal behavior of the model with the reference parameters as in Fig. 1 is shown by Fig. 2*A* and *B*. The time course of the free running V (Fig. 2*A*) shows two types of oscillations, fast cycles (about 4 sec) by electrocoupling with small concentration changes as described by Gradmann et al. (1993), and slower cycles (about 50 sec) which comprise concentration changes. With respect to the V oscillations in Fig. 2*B*, these changes of cytoplasmic concentrations are reflected by small but significant oscillations of E_{Cl}, E_K and E_{Sy}. The fast oscillations occur during the period of release of K^+ and Cl^- within the slow cycle and are missing during the period of uptake of K^+ and Cl^- within the slow cycle when V stays at the negative plateau.

Figure 2*C* shows the effect of the area/volume ratio, $R_{A:V}$, on the behavior of the model. Doubling $R_{A:V}$ (the only difference between Fig. 2*C* and *A*, *B*) causes exact doubling of the frequency of the slow oscillations which involve changes in $c_{K,c}$ and in $c_{Cl,c}$ as seen by the traces for E_{Cl}, E_K and E_{Sy}. In contrast, $R_{A:V}$ does not affect the frequency of the fast oscillations which operate at constant E_{Cl}, E_K and E_{Sy} (Gradmann et al., 1993). There is only a smaller number of fast cycles (five in 2*B* instead of ten under reference conditions 2*A* and *B*) during the (50%) shorter period of ion release in Fig. 2*C* compared to 2*A* and *B*. One reason for the choice of the reference parameters was to present the two types of oscillations as

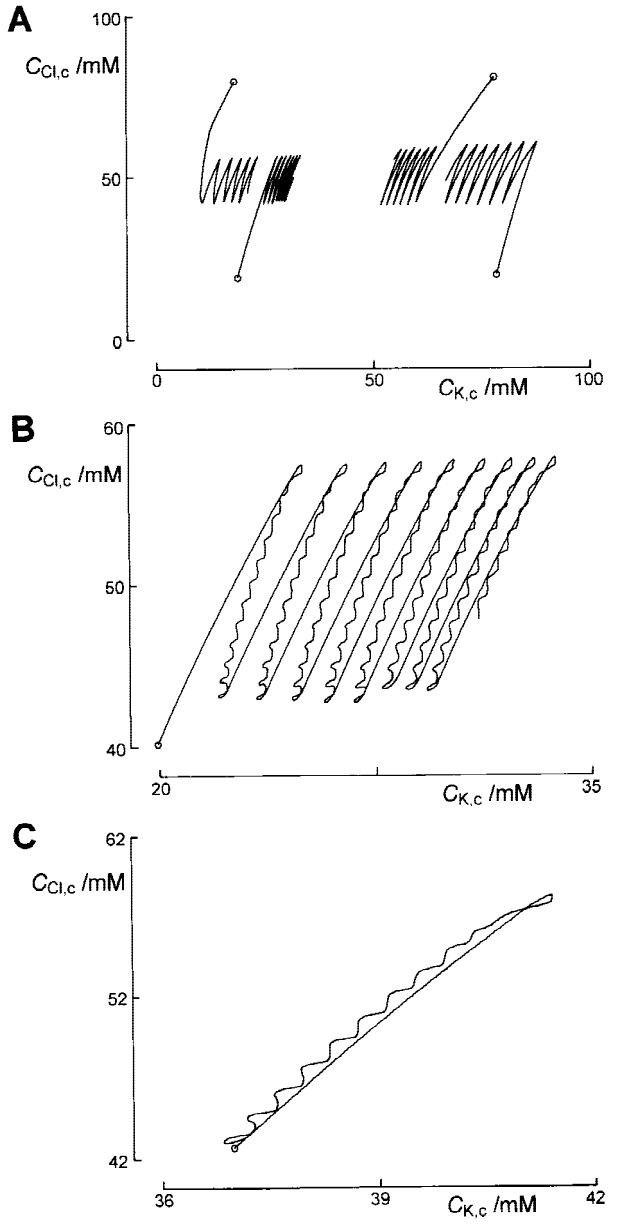

Fig. 5. Changes in $c_{K,c}$ and $c_{Cl,c}$ of model with parameters as in Fig. 1 with different start concentrations; circles mark beginnings; (*A*) Development during 400 sec for four different start conditions (circles) far from stable state, showing convergence towards stable oscillations; (*B*) Detail showing that the stepwise change in amplitudes (as in the tracing in Fig. *A* but starting from 20 mM $c_{K,c}$ and 40 mM $c_{Cl,c}$) of the slow cycles is due to an integer change of fast cycles (compare Fig. 2); (*C*) With start concentrations 37 mM $c_{K,c}$ and 42.8 mM $c_{Cl,c}$, the systems readily enters stable oscillations; entire trace represents 1,000 sec comprising 19 coinciding slow cycles of about 51 sec duration as in Fig. 2.

nearly uncoupled phenomena and clearly distinct by the different frequencies. In fact, the two phenomena would merge if we were to increase the area/volume ratio further.

If ion concentrations, and therefore E_K, E_{Cl} and E_{Sy} are forced constant in this model, the slow oscillations are absent and the fast oscillations may remain. The voltage courses in Fig. 3 illustrate the behavior of the model under these conditions. They show that the rate constants for gating of the transporters *Pu*, K_o, K_i, and *Sy* have only some minor effect on the shape of the oscillations and very little effect on the frequency, whereas *Cl* seems essential for the fast oscillations, because the gating velocity of *Cl* has an almost proportional effect on the frequency. At increasing velocity, the proportionality vanishes when *Cl* reaches a gating velocity comparable to the other transporters. This property can be explained by the requirement of a time lag for oscillations in a first-order-differential equation system. In our system, the major delay lies in the slow transition $i_2 \rightarrow a \rightarrow i_1$ *in Cl* which occurs when *V* becomes more negative. In comparison, the other transitions can be regarded as instantaneous and synchronized to the membrane voltage. Furthermore, the intermediate position of the active state of *Cl* is crucial: during a positive change (rise) of *V* from $V << 0$, *Cl* will be transiently activated from i_1 to *a* and support further rising of *V*, but then *Cl* will enter i_2, so that the effect of the Cl^- conductance decreases again and reduces the impact of *Cl* on *V*, with the result that *V* will become more negative again. With considerable delay, *Cl* will return now from i_2 to *a*, and the Cl^- current will drive *V* more positive again. Tracing D in Fig. 3 shows that these fast oscillations take place only if the timing of the system is correct (within about an order of magnitude) and if the contribution of E_{Cl} to *V* is within an appropriate range. For small $c_{Cl,c}$, the Cl^- (outward) current becomes small and its effect on *V* is weak. In this case, *V* stays rather negative and drives salt uptake through K_i and *Sy*. When $c_{Cl,c}$ is large E_{Cl} will become more positive and g_{Cl} larger and the fast *Cl*-dependent oscillations take place. Even if these oscillations depend strongly on the correct timing, and therefore on our somewhat arbitrary parameter set, it is quite probable that such a configuration can exist in real cells, because these fast oscillations are closely related to the previously reported voltage oscillations (Gradmann et al., 1993) which have been observed.

The slow oscillations which reflect switching between states of salt release and salt uptake, can be discussed separately, if we allow the system to perform concentration changes, but assume that the transporters attain their voltage-sensitive activities not by gating relaxations but immediately by Eqs. 9 and 11. In this case, the fast oscillations are absent and the slower ones remain unaffected by absolute values of the *k*'s, of course. Figure 4 shows this behavior for the reference parameters in Fig. 1. The behavior of this system can be described as follows.

If *V* is sufficiently negative, K_i and *Sy* will be active, catalyzing uptake of K^+ and $(Cl^-\text{-}2H^+)^+$. The increasing $c_{K,c}$ and $c_{Cl,c}$ result in more negative E_K and E_{Sy}, thus

Table. Relative differential quotients $(dydx)/y$ in ‰ of model in Fig. 1

	y	T_{eyel}	T_{hyp}	T_{dep}	T_{osc}	A_{osc}	$E_{K,mx}$	$E_{K,mn}$	$E_{Cl,mx}$	$E_{Cl,mn}$	$E_{Sy,mn}$	$E_{Sy,mn}$	V_{mx}	V_{mn}
x	Ref.	52.17	18.27	33.90	3.80	124.75	−91.66	−94.67	103.14	95.47	56.68	49.01	21.33	−181.30
E_{Pu}	−400	−368	330	−1000	555	−49	−1	1	−21			94	−747	−12
g_{Pu}	1.0	317	−168	801	2284	57		6	12			−54	482	7
$k_{\mathrm{a,Pu}}$	1.0	−14	−2	−28	−13	3		1				−1		
$k_{\mathrm{i,Pu}}$	10.0	1	9	−127	255	4	−2			−1	2	1	68	
g^0_{Ko}	0.1	1	14	−2	−5	−5								
$k_{a,Ko}$	1.0	4	10	−2	13	−2							−35	
$k_{i,Ko}$	1.0	1	−10	5	29								48	
g^0_{Ki}	0.2	−26	2	−63	103	−2			−1	−1	1	6	9	−1
$k_{a,Ki}$	1.0	1	2	3	47	2					1	1	34	
$k_{\mathrm{i,Ki}}$	100	16	3	38	187	4					1	−1	−21	
g_{Sy}	0.65	23	30	62	1871	32	−3	−4	−1	−7	19	32	303	−5
$k_{a,Sy}$	1.0	18	−2	−1	208	4					1		46	
$k_{i,Sy}$	1.0		−4	2	21	1							39	
g^0_{Cl}	0.1	−18	64	−69	63	−8	−1	−1	−3	−3	9	14	34	−9
k_{a1}	25	.27	53	−80	276	−1		−1	−3	−2	6	13	−9	−1
k_{i1}	0.5	59	−73	161	76	10	−1	1	3			−13	27	1
k_{a2}	0.1	−32	−30	67	−8	−3	−1			−1	3		49	
k_{i2}	1.0	−4	−16	−4	−47	4							22	

Reference parameters x in first two columns; constant external concenatrations: $c_{K,1} = c_{Cl,l} = 1$ mM, $\mathrm{pH}_1 = 6$; $\mathrm{pH}_c = 7.3$; cytoplasmic start concentrations: $c_{K,c} = c_{Cl,c} = 40$ mM; T_{cycl}: duration of slow cycle; T_{hyp}: time span when $V < (V_{\mathrm{mx}} + V_{\mathrm{mn}})/2$; $T_{dep} = T_{cyst} - T_{hyp}$; T_{osc}: duration of last fast cycle during T_{dep}; A_{osc}: amplitude of last fast cycle during T_{dep}; $V(E)_{\mathrm{mx}}$ and $V(E)_{mm}$: maximum and minimum (equilibrium) voltages; g^0: conductance at symmetrical 1 mM substrate; k_a and k_i; transition probabilities for activation and inactivation at $V = 0$; units: T/s; A, E, V/mV; $\mathrm{g}/S{\cdot}\mathrm{m}^{-2}$; $g^0/S{\cdot}m^{-2}\mathrm{mM}^{-1}$; k/s^{-1}; $|(dy/dx)/y| < 0.5$‰: –.

causing a positive feedback for increasingly negative V. During the increase in $c_{Cl,c}$, however, the increasing driving force for Cl^-, $V - E_{Cl}$, and the increasing *GHK*-conductance for inward current (efflux) of Cl^-, will keep this diverging behavior in check. These synergistic increases of $V - E_{Cl}$ and of G_{Cl} will drive the system to a threshold when the hyperpolarization due to positive feedback through K_i and Sy is balanced by the depolarization due to Cl ($dV/dt = 0$). From this threshold, Cl will activate in a regenerative mode with a positive step of V. The following salt loss at positive V causes E_{Cl} to grow more negative again, thus causing V to become more negative as well. This trend will slow down as Cl enters i_1 by the voltage-sensitive ratio k_{i1}/k_{a1} of Cl, and V comes to a temporal rest again in the negative V range until initiation of a new cycle. This description is, of course, taken to extremes by allowing the transporters to equilibrate immediately. On the other hand, the events during a slow oscillation with the reference parameter set are similar, though more gradual.

Long-Term Behavior

Due to intrinsic properties the model never diverges to the V limits of E_{Pu} or E_{Cl} but V converges either to a stable resting voltage or to stable oscillations. Figure 5*A* shows that from excessively large and small start values of $c_{K,c}$ and $c_{Cl,c}$ the system with reference parameters converges to stable slow oscillations of $c_{K,c}$ (between about 37 and 42 mM) and of $c_{Cl,c}$ (between about 42 and 58 mM). The corresponding V oscillations are not illustrated in Fig. 5. It is pointed out that the modified model with steady-state occupancies (Fig. 4) converges to similar ion concentrations. This means that long-term conditions are dominated by the slow oscillations and not by gating.

The slow oscillations of c_{Kc} and of $c_{Cl,c}$ are well in phase. This feature reflects the fact that K^+ uptake through the K_i and Cl^- uptake through Sy are driven simultaneously by the negative V plateau during the slow oscillations. In contrast, substantial loss of K^+ and Cl^- takes place during the periods of considerably more positive V which results in net release of K^+ and Cl^- during these fast oscillations. It is pointed out that the differences of the amplitudes in $c_{Cl,c}$ and in $c_{K,c}$ are electrically neutralized by corresponding fluxes of H^+. These H^+ fluxes, however, can be expected to have no osmotic consequences because of cytoplasmic pH buffering.

A small, stepwise decrease in the amplitudes of $c_{Cl,c}$ and $c_{K,c}$ can be identified in Fig. 5*A*, i.e., before the last

three cycles in the tracing which starts at 20 mM $c_{K,c}$ and 20 mM $c_{Cl,c}$. Increased resolution of this detail (Fig. 5*B*) shows that this phenomenon consists of a down-step by one of the number of fast cycles within the time span of salt release.

When 37 mM $c_{K,c}$ and 42.8 mM $c_{Cl,c}$ are used for start conditions, all the 19 cycles within a run of 1,000 sec coincide (Fig. 4*C*), i.e., the oscillations are stable without further drift. The sensitivity of the system in this stable dynamic state is characterized in some detail by the matrix of relative differential quotients (Table), which are in fact the absolute change dy/dx of a state variable y with a parameter x, in relation to the value of y. The numerical results need to be taken with precaution because they reflect only the system with the specific parameters in the first two columns (x), and the y-values for time spans and for voltages cannot be compared directly. Nevertheless some qualitative features can be recognized in this table:

(1) The most dramatic effects are due to changes in E and g of the pump, followed by changes in g of the symporter, and by the rate constants of *Cl*.

(2) The effects on the time courses are larger than the effects on the voltages. This may be due to the fact that in reaction kinetic terms, voltages correspond only to the logarithm of a concentration, whereas apparent rate constants are proportional to the ligand concentrations and enter velocities directly.

(3) Antagonistic k's might be expected to have antagonistic effects, i.e., $dy(k_a)/dy(k_i) \approx -1$. This rule cannot be confirmed by the results for $y = T$, because—despite of secondary effects—an increase in k will primarily accelerate, causing intrinsic decreases of one or several T.

(4) In particular, such rules do not hold for small effects, here, where e.g., small increases in either k_a or k_i of the inward rectifier may slightly retard the slow oscillations—and the fast ones as well.

Figure 6 shows that minor changes of the model parameters can cause the system to converge to a stable state where the slow oscillations with intrinsic changes in $c_{K,c}$ and $c_{Cl,c}$ are absent and only the fast oscillations persist which comprise no intrinsic changes in $c_{K,c}$ and $c_{Cl,c}$. This feature is documented by Fig. 6*A* and *B* showing that differences in $c_{K,c}$ and $c_{Cl,c}$ (as imposed by a change in the area/volume ratio) do not affect frequency or shape of these oscillations.

Figure 7 illustrates that the system can also converge to a stable steady-state without any oscillations. This behavior is typically accomplished by a narrowing of the range of driving forces, here by choosing a more positive E_{Pu} which forces the system to operate more closely to thermodynamic equilibria (Glansdorf & Prigogine, 1971). This rule has been confirmed explicitly for membrane models with electrical interaction between batter-

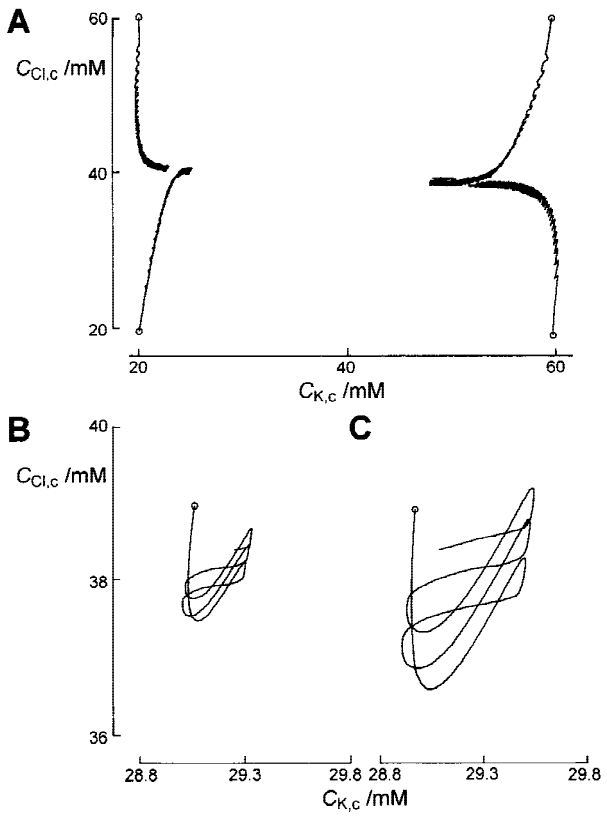

Fig. 6. Changes in $c_{K,c}$ and $c_{Cl,c}$ of model with parameters as in Fig. 1 except $g_{Sy,mx} = 1$ S m^{-2}, and $k_{Sy,a} = 0.05$ sec^{-1} at zero voltage showing absence of slow oscillations and continuous fast oscillations; circles mark beginnings; (*A*) Temporal development during 200 sec with four different start concentrations of $c_{K,c}$ and $c_{Cl,c}$;(*B*) Same parameters as in *A* but with start parameters (29 mM $c_{K,c}$ and 39 mM $c_{Cl,c}$) closer to stability; development over 10 sec from start; (*C*) Same parameters as in *B* except twice the area/volume ratio ($2 \cdot 10^6$ m^{-1}), revealing — in comparison with (*B*) — doubling of concentration amplitudes at virtually constant frequency and shape.

ies with different driving forces (Buschmann & Gradmann, 1997). When the system does approach a real steady-state such as in Fig. 7, E_K and V will eventually coincide at a stable level, and the currents through *Sy* and *Cl* will adjust as to yield zero net flux of Cl^-.

As already mentioned above, the model parameters have not been adjusted here to simulate experimental phenomena as naturalistically as possible. Dreyer and Hedrich (1996) have carried out such an attempt using the preceding version (Gradmann et al., 1993) of the model. However, such numerical approaches are expected to be misleading because they leave too little room for other essential processes, such as ligand gating or $c_{Ca,c}$ related V oscillations (Mahr et al., 1997). Nevertheless, the main phenomena described here are not mere speculations but are qualitatively paralleled in some detail by electrophysiological observations, e.g., in guard cells, where alternating periods of stable and os-

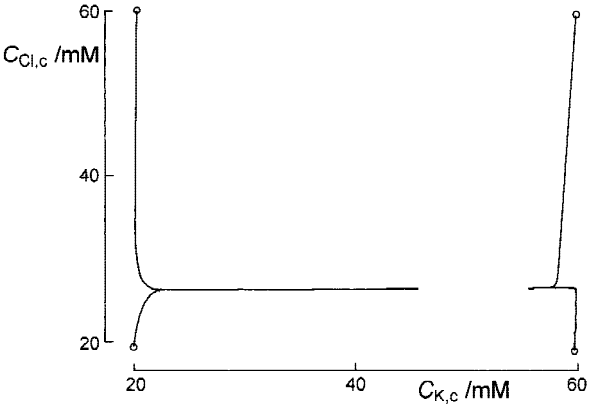

Fig. 7. Changes in $c_{K,c}$ and $c_{Cl,c}$ of model with parameters as in Fig. 4, except $E_{Pu} = -200$ mV and $g_{Pu} = 3$ S m^{-2}, example for approach towards nonoscillating, steady-state concentrations of 55.0 mM $c_{K,c}$, 27.4 mM $c_{Cl,l}$, and $V = -102$ mV; traces represent converging development over 1,000 sec from four different start concentrations (circles).

cillating voltages are observed (Thiel et al., 1992; Blatt & Thiel 1994) or in *Acetabularia* where turgor and frequency of spontaneous electrical oscillations do correlate strikingly (Wendler et al., 1983).

Conclusions

In plant cells, interaction of the major electroenzymes with internal ion concentrations converges to a stable osmotic state, where ion concentrations may oscillate around equilibrium values. The intrinsic convergence of this new type of oscillations is an important prerequisite for other physiological mechanisms of osmotic regulation.

References

Blatt, M.R., Thiel, G. 1994. K^+ channels of stomatal guard cells: bimodal control of the K^+ inward-rectifier evoked by auxin. *The Plant Journal* **5:**55–68

Buschmann, P., Gradmann, D. 1997. Minimal model for oscillations of membrane voltage in plant cells. *J. Theoret. Biol.* **188:**323–332

Dreyer, I., Hedrich, R. 1996. Action Potentials in Guard Cells — the Molecular Basis of Oscillations. Botanikertagung, P-9.060, 25.-31.8. Düsseldorf

Glansdorf, P., Prigogine, I. 1971. Thermodynamic Theory of Structure, Stability and Fluctuations. John Wiley, New York

Gradmann, D., Blatt, M.R., Thiel, G. 1993. Electrocoupling of ion transporters in plants. *J. Membrane Biol.* **136:**327–332

Gradmann, D., Buschmann, P. 1996. Electrocoupling causes oscillations of ion transporters in plants. *In:* Vistas on Biorhythmicity, H. Greppin, R. Degli Agosti, and M. Bonzon, editors. pp. 239–268. University of Geneva

Mahr, M., Schuster, S., Brumen, M., Heinrich, R. 1997. Modelling the interrelations between calcium oscillations and ER membrane potential oscillations. *Biophysical Chemistry* **68:**221–239

Tarantola, A., 1987. Inverse Problem Theory — Methods for Data Fitting and Model Parameter Estimation, Elsevier, Amsterdam

Thiel, G., Gradmann, D. 1994. Electrophysiology of stomata. *Progress in Botany* **55:**59–78

Thiel, G., MacRobbie, E.A.C., Blatt, M.R. 1992. Membrane transport in stomatal guard cells. The importance of voltage control. *J. Membrane Biol.* **126:**1–18

Wendler, S., Zimmermann, U. Bentrup, F.-W. 1983. Relationship between cell turgor pressure, electrical membrane potential, and chloride efflux in *Acetabularia mediterranea*. *J. Membrane Biol.* **72:**75–84